Table IV. Crystallographic Data for **6**-$(THF)_4$ and **13a**

chem formula	$[Cp^*Me_3W{=}NNH]_2[\mu\text{-}Mg(THF)_4]^a$	$[Cp^*Me_3W]_2(\mu\text{-}N)$
a, Å	12.380 (6)	8.390 (4)
b, Å	15.252 (6)	20.341 (6)
c, Å	30.618 (8)	8.733 (4)
β, deg	97.91 (3)	117.83 (2)
V, Å^3	5726 (7)	1318 (2)
Z, molecules/cell	4	2
MW	1099.14	742.37
space group (No. 14)	$P2_1/n$	$P2_1/c$
λ, Å	0.710 73	0.710 73
ρ(calcd), g/cm^3	1.275	1.870
μ, cm^{-1}		89.21
R^b	0.082	0.057
$R_w{}^c$	0.132	0.063

[a] The structure of **6**-$(THF)_4$ could not be refined adequately, although the connectivity was established unequivocally. Full details are provided in the supplementary material. [b] $R = \sum||F_o| - |F_c||/\sum|F_o|$. [c] $R_w = [\sum w(|F_o| - |F_c|)^2/\sum wF_o^2]^{1/2}$.

full-matrix least-squares refinement was based on 2011 reflections ($I > 3.00\sigma(I)$) and 108 variables and used the TEXSAN crystallographic software package from the Molecular Structure Corp. The final refinement converged with final $R = 0.057$ and $R_w = 0.063$. The maximum and minimum peaks on the final Fourier difference map corresponded to 2.29 and -2.08 e/Å^3, respectively. Crystal data can be founde in Table IV.

Acknowledgment. R.R.S. thanks the National Institutes of Health for support through Grant GM 31978 and T.E.G. thanks the National Science Foundation for a graduate fellowship. We thank M. G. Vale for quantifying the bulk hydrolysis of **9** and determining the structure of **13a** and Dr. W. M. Davis of the MIT Chemistry Department X-ray Diffraction Facility for valuable assistance with the solution of **6**-$(THF)_4$. We also thank J. F. Payack, Jr., for the preparation and analysis of $Cp^*Me_3W{=}NN(SiMe_3)_2$.

Supplementary Material Available: A labeled ORTEP drawing of **13a**, tables of final positional and thermal parameters for **13a**, a description of the X-ray study of **6**-$(THF)_4$, and tables of final positional and thermal parameters for **6**-$(THF)_4$ (11 pages); listings of final observed and calculated structure factors for **13a** and **6**-$(THF)_4$ (34 pages). Ordering information is given on any current masthead page.

(58) Payack, J. F., Jr. S.M. Thesis, MIT, 1987.

Contribution from the School of Chemical Sciences, University of Illinois at Urbana-Champaign, 505 South Mathews Avenue, Urbana, Illinois 61801

Characterization of Silica-Supported Osmium Carbonyl Clusters by Magic-Angle-Spinning Carbon-13 NMR Spectroscopy

Thomas H. Walter, Greg R. Frauenhoff, John R. Shapley, and Eric Oldfield*

Received June 5, 1991

We report the carbon-13 magic-angle-spinning nuclear magnetic resonance (NMR) spectra of silica-supported $Os_3(^{13}CO)_{12}$ samples prepared in several different ways. Our results yield both the isotropic chemical shift and the principal components of the chemical shift tensor for each carbonyl resonance. Spectra have been assigned by comparison to solution NMR spectra of a variety of osmium carbonyl clusters that are models for the proposed surface-attached structures: $HOs_3(CO)_{10}(OR)$ (R = CH_3, C_6H_5, $SiEt_3$), $HOs_3(CO)_{10}(O_2CH)$, $Os_3(CO)_{10}(OCH_3)_2$, and $[Os(CO)_3Cl_2]_2$. Spectra of samples prepared by impregnation of silica with a solution of $Os_3(^{13}CO)_{12}$ provide evidence for a physisorbed $Os_3(CO)_{12}$ species undergoing fast isotropic motion. For samples prepared by refluxing $Os_3(^{13}CO)_{12}$ and SiO_2 in *n*-octane, a spectrum containing five distinct resonances is observed, consistent with a $HOs_3(CO)_{10}(OSi{\equiv})$ species having C_s symmetry. The chemical shift anisotropy parameters measured for these resonances at 20 °C suggest that this species is undergoing rapid (≫32 kHz) large-angle (90-120°) rotational jumps. Spectra of samples prepared by vacuum pyrolysis (200 °C) are consistent with Os(II) carbonyl species that are immobile on the 10^{-5}-10^{-4}-s time scale. These results demonstrate the utility of ^{13}C NMR spectroscopy for studying the structures and dynamics of supported metal carbonyl clusters.

Supported metal complexes have been widely investigated both as novel catalysts and as models for the supported metal crystallites that are commonly used as catalysts in petroleum refining.[1-5] In contrast to supported metal crystallites, supported metal complexes may provide uniform catalytic centers which are more readily analyzed, thus allowing the identification of important catalyst properties through systematic synthesis and characterization.[3,5] However, determining the detailed structures of supported complexes has proven to be a challenging task, and a wide array of techniques have been applied to the problem.[3,6] While vibrational spectroscopies (infrared, Raman, and inelastic electron tunneling) have been most widely used to date, there has been a growing interest in the use of extended X-ray absorption fine structure (EXAFS)[7,8] and magic-angle-spinning nuclear magnetic resonance (MAS NMR) spectroscopies.[9] Despite the well-known utility of ^{13}C NMR spectroscopy for characterizing metal complexes in solution, ^{13}C NMR spectroscopy has not yet been widely exploited to study supported metal complexes. This may be, in part, because special techniques must often be used. Isotopic enrichment is frequently required to obtain useful signal-to-noise ratios in a reasonable period of time, and magic-angle spinning and high-power proton decoupling are generally necessary to obtain high resolution. Many samples also require the use of sealed sample holders to prevent contact with air.[9-11] Despite these compli-

(1) Yermakov, Yu. I.; Kuznetsov, B. N.; Zakharov, V. A. *Catalysis by Supported Complexes*; Elsevier: Amsterdam, 1981.
(2) Bailey, D. C.; Langer, S. H. *Chem. Rev.* **1981**, *81*, 109.
(3) Hartley, F. R. *Supported Metal Complexes*; Reidel: Dordrecht, Holland, 1985.
(4) Gates, B. C. In *Metal Clusters*; Moskovits, M., Ed.; Wiley: New York, 1986; p 283.
(5) Basset, J. M.; Choplin, A. *J. Mol. Catal.* **1983**, *21*, 95.
(6) Gates, B. C.; Lieto, J. *CHEMTECH* **1980**, *10*, 248.
(7) Evans, J. *Spectrochim. Acta* **1987**, *43A*, 1511.
(8) Duivenvoorden, F. B. M.; Koningsberger, D. C.; Uh, Y. S.; Gates, B. C. *J. Am. Chem. Soc.* **1986**, *108*, 6254.
(9) (a) Fischer, A. B.; Bruce, J. A.; McKay, D. R.; Maciel, G. E.; Wrighton, M. S. *Inorg. Chem.* **1982**, *21*, 1766. (b) Hanson, B. E.; Wagner, G. W.; Davis, R. J.; Motell, E. *Inorg. Chem.* **1984**, *23*, 1635. (c) Liu, D. K.; Wrighton, M. S.; McKay, D. R.; Maciel, G. E. *Inorg. Chem.* **1984**, *23*, 212. (d) McKenna, W. P.; Eyring, E. M. *J. Mol. Catal.* **1985**, *29*, 363. (e) Komoroski, R. A.; Magistro, A. J.; Nicholas, P. P. *Inorg. Chem.* **1986**, *25*, 3917. (f) Prigano, A. L.; Trogler, W. C. *J. Am. Chem. Soc.* **1987**, *109*, 3586. (g) Hedden, D.; Marks, T. J. *J. Am. Chem. Soc.* **1988**, *110*, 1647. (h) Dahmen, K.-H.; Hedden, D.; Burwell, R. L.; Marks, T. J. *Langmuir* **1988**, *4*, 1212. (i) Weiss, K.; Lossel, G. *Angew. Chem., Int. Ed. Engl.* **1989**, *28*, 62.

0020-1669/91/1330-4732$02.50/0

cations, it has been shown that MAS ^{13}C NMR spectroscopy can provide incisive information on the structures of supported mononuclear metal complexes.[9,10] There have also been a few studies of supported metal clusters.[11] To further explore the utility of NMR spectroscopy in characterizing supported metal clusters, we have examined the surface species formed by the reaction of $Os_3(CO)_{12}$ and silica. A preliminary account of this work has been published.[12]

The surface organometallic chemistry of $Os_3(CO)_{12}$ on silica and alumina has been extensively investigated.[13-15] Room-temperature impregnation of hydroxylated silica or alumina with a solution of $Os_3(CO)_{12}$ has been shown to produce only a physical mixture of $Os_3(CO)_{12}$ and support.[13,14] After the system is heated at 100–150 °C, however, a covalently bound complex is formed.[13,15] Infrared spectroscopy indicates that this complex has one of the structures shown in **1**–**3**. Unfortunately, the IR spectra of homogeneous models for these structures are too similar to allow an unambiguous assignment.[13] Gas evolution measurements, however, indicate that the reaction between $Os_3(CO)_{12}$ and hydroxylated silica or alumina produces 2 mol of CO/mol of $Os_3(CO)_{12}$, but only traces of H_2, suggesting the formation of structure **1** via oxidative addition of a surface hydroxyl group:[13]

1

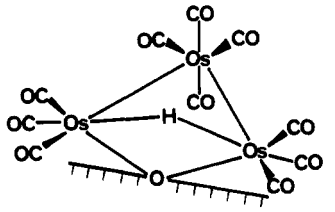

2

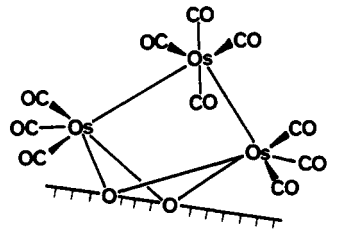

3

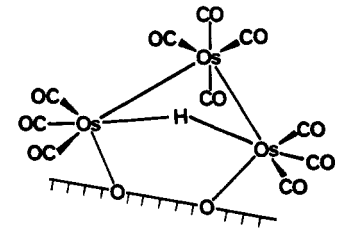

$$Os_3(CO)_{12} + HOSi{\equiv} \rightarrow HOs_3(CO)_{10}(OSi{\equiv}) + 2CO$$

Prolonged heating at 150–200 °C leads to breakup of the triosmium framework, with simultaneous oxidation by surface hydroxyls, to give $Os^{II}(CO)_n$ (n = 2, 3) species.[13,15] Samples containing these mononuclear species have been shown to be Fischer–Tropsch catalysts with a high selectivity for methane[13,15,16] and also catalyze the hydrogenation of ethylene.[15] In addition, samples containing the supported triosmium cluster have been reported to be catalysts for olefin isomerization, with the cluster framework remaining intact under the reaction conditions.[17]

Because of the air stability of these samples[13] and the relatively well-defined nature of the supported cluster, this system has been characterized by a large number of techniques. There have been several IR studies,[13,14,18,19] as well as reports of investigations using inelastic electron tunneling[20] and Raman spectroscopies.[19,22] X-ray photoelectron spectroscopy has been used to determine Os oxidation states,[16] and laser Raman spectroscopy, to provide evidence for Os–Os bonds.[22] It has been shown that transmission electron microscopy can be used to observe uniform <1-nm scattering centers, attributed to trimeric $Os(CO)_3$ units.[16,23] This system has also been extensively characterized by osmium K-edge EXAFS spectroscopy.[7,8,13,19,24] Although the EXAFS data have provided new information on the mononuclear fragments resulting from degradation of the triosmium cluster,[8] it has not allowed the distinction among structures **1**–**3** for the chemisorbed cluster, the data being consistent with all three. In this report, we describe the first detailed ^{13}C NMR investigation of supported $Os_3(CO)_{12}$. By comparing the spectrum of the silica-supported triosmium cluster with the spectra of a variety of model compounds of the forms $HOs_3(CO)_{10}(OR)$, $Os_3(CO)_{10}(OR)_2$, and $HOs_3(CO)_{10}(O_2CR)$, we show that structure **1** may be confidently assigned to this species. We also present evidence suggesting that this cluster undergoes rapid (≫32 kHz) large-angle rotational jumps, on the basis of our observation of a partially averaged chemical shift anisotropy for each of the carbonyl ligands.

Experimental Section

Chemical Aspects. The preparation of ^{13}C-enriched $Os_3(CO)_{12}$ has been described previously.[25] $H_2Os_3(^{13}CO)_{10}$ was prepared from $Os_3(^{13}CO)_{12}$ and H_2 at 120 °C in octane, by following the procedure of Knox et al.[26] The crude product was purified by chromatography on silica and recrystallized from chloroform/hexane (1:1 v/v). $HOs_3(^{13}CO)_{10}(OC_6H_5)$ was prepared from $Os_3(^{13}CO)_{12}$ and phenol in refluxing xylene, as described by Azam.[27] The product was isolated from the reaction mixture by preparative thin-layer chromatography and recrystallized from chloroform/hexane. $HOs_3(^{13}CO)_{10}(OOCH)$ was prepared from $H_2Os_3(^{13}CO)_{10}$ as described by Shapley et al.[28] and was recrystallized from CH_2Cl_2 at −15 °C. $[Os(CO)_3Cl_2]_2$ was prepared from $Os(CO)_4Cl_2$ in refluxing chloroform, as described by Psaro and Dossi,[29] and recrystallized from CCl_4. $Os(CO)_4Cl_2$ was prepared by treating $OsCl_3$ with CO (65 atm) for 22 h at 155 °C in a stainless steel autoclave. $[Os(CO)_3Cl_2]_2$ was enriched in ^{13}C by exchange with [99% ^{13}C]-CO (Monsanto Research Corp., Miamisburg, OH) in chlorobenzene at 95 °C for 5 days. Other model compounds were prepared as follows:

$HOs_3(^{13}CO)_{10}(OCH_3)$.[30] $Os_3(^{13}CO)_{12}$ (265 mg, 0.292 mmol) and

(10) Walter, T. H.; Thompson, A.; Keniry, M.; Shinoda, S.; Gutowsky, H. S.; Brown, T. L.; Oldfield, E. *J. Am. Chem. Soc.* **1988**, *110*, 1065.
(11) (a) Robbins, J. L. *J. Phys. Chem.* **1986**, *90*, 3381. (b) Hanson, B. E. In *Advances in Dynamic Stereochemistry*; Geilen, M. F., Ed.; Freund: London, 1985; p 53. (c) Hasselbring, L.; Puga, J.; Dybowski, C.; Gates, B. C. *J. Phys. Chem.* **1988**, *92*, 3934.
(12) Walter, T. H.; Frauenhoff, G. R.; Shapley, J. R.; Oldfield, E. *Inorg. Chem.* **1988**, *27*, 2563.
(13) (a) Besson, B.; Moraweck, B.; Smith, A. K.; Basset, J. M.; Psaro, R.; Fusi, A.; Ugo, R. *J. Chem. Soc., Chem. Commun.* **1980**, 569. (b) Smith, A. K.; Besson, B.; Basset, J. M.; Psaro, R.; Fusi, A.; Ugo, R. *J. Organomet. Chem.* **1980**, *192*, C31. (c) Psaro, R.; Ugo, R.; Zanderighi, G. M.; Besson, B.; Smith, A. K.; Basset, J. M. *J. Organomet. Chem.* **1981**, *213*, 215.
(14) Collier, G.; Hunt, D. J.; Jackson, S. D.; Moyes, R. B.; Pickering, I. A.; Wells, P. B.; Simpson, A. F.; Whyman, R. *J. Catal.* **1983**, *80*, 154.
(15) Deeba, M.; Gates, B. C. *J. Catal.* **1981**, *67*, 303.
(16) Knozinger, H.; Zhao, Y.; Tesche, B.; Barth, R.; Epstein, R.; Gates, B. C.; Scott, J. P. *Faraday Discuss. Chem. Soc.* **1981**, *72*, 53.
(17) (a) Barth, R.; Gates, B. C.; Zhao, Y.; Knozinger, H.; Hulse, J. *J. Catal.* **1983**, *82*, 147. (b) Li, X. J.; Onuferko, J. H.; Gates, B. C. *J. Catal.* **1984**, *85*, 176.
(18) Knozinger, H.; Zhao, Y. *J. Catal.* **1981**, *71*, 337.
(19) Cook, S. L.; Evans, J.; McNulty, G. S.; Greaves, G. N. *J. Chem. Soc., Dalton Trans.* **1986**, 7.
(20) Hilliard, L. J.; Gold, H. S. *Appl. Spectrosc.* **1985**, *39*, 124.
(21) Alexiev, V. D.; Binsted, N.; Evans, J.; Greaves, G. N.; Price, R. J. *J. Chem. Soc., Chem. Commun.* **1987**, 395.
(22) Deeba, M.; Steusand, B. J.; Schrader, G. L.; Gates, B. C. *J. Catal.* **1981**, *69*, 218.
(23) Schwank, J.; Allard, L. F.; Deeba, M.; Gates, B. C. *J. Catal.* **1983**, *84*, 27.
(24) Cook, S. L.; Evans, J.; Greaves, G. N. *J. Chem. Soc., Chem. Commun.* **1983**, 1287.
(25) Walter, T. H.; Reven, L.; Oldfield, E. *J. Phys. Chem.* **1989**, *93*, 1320.
(26) Knox, S. A. R.; Koepke, J. W.; Andrews, M. A.; Kaesz, H. D. *J. Am. Chem. Soc.* **1975**, *97*, 3942.
(27) Azam, K. A.; Deeming, A. J.; Kimber, R. E.; Shukla, P. R. *J. Chem. Soc., Dalton Trans.* **1976**, 1853.
(28) Shapley, J. R.; St. George, G. M.; Churchill, M. R.; Hollander, F. J. *Inorg. Chem.* **1982**, *21*, 3295.
(29) Psaro, R.; Dossi, C. *Inorg. Chim. Acta* **1983**, *77*, L25.

methanol (30 mL, distilled from $Mg(OCH_3)_2$) were placed in an autoclave (300-mL capacity). After several partial evacuations and flushes with N_2, the autoclave was charged to slightly over atmospheric pressure with N_2, sealed, and placed in an oil bath maintained at 126 °C. After 13 h, the autoclave was cooled to room temperature and opened, and after the methanol solvent was stripped, the crude residue was chromatographed on silica using hexane as an eluant. The product, which moved as a yellow band, was collected and recrystallized from CH_2Cl_2/*n*-pentane at −15 °C (56% yield).

$Os_3(^{13}CO)_{10}(OCH_3)_2$. Attempts were made to prepare this complex by reaction of $HOs_3(^{13}CO)_{10}(OCH_3)$ with methanol in an autoclave at temperatures from 125 to 145 °C and reaction times of 24–30 h, but these conditions gave poor yields (5–15%). Consequently, $Os_3(^{13}CO)_{10}(OCH_3)_2$ was prepared from an *n*-octane solution of $Os_3(CO)_{10}(OCH_3)_2$ (obtained as a byproduct in the synthesis of $Os_3(CO)_{12}$ from OsO_4 and CO in methanol[31]) and ^{13}CO in a pressure bottle at 123 °C for 48 h. After cooling and removal of the solvent, the residue was purified on silica TLC plates using hexane eluant. The single yellow band of $Os_3(^{13}CO)_{10}(OCH_3)_2$ was collected and the product recrystallized from CH_2Cl_2.

$HOs_3(^{13}CO)_{10}(OSiEt_3)$. The following synthesis is based on that described by Calvert.[32] To $H_2Os_3(^{13}CO)_{10}CH_2$[33] (157.5 mg, 0.181 mmol) in CH_2Cl_2 (10 mL, distilled from P_4O_{10}) was added Et_3SiOH (360 μL). The solution was stirred at room temperature for 4 days. It was concentrated and loaded onto silica TLC plates, after which a bright yellow band eluted with hexanes (R_f = 0.59). This band was recovered, and the product was recrystallized from pentane at −15 °C to give $HOs_3(^{13}CO)_{10}(OSiEt_3)$ as orange-yellow blocks (50% yield).

$Os_3(^{13}CO)_{12}/SiO_2$. Silica-supported $Os_3(^{13}CO)_{12}$ samples were prepared from 60% ^{13}C-enriched $Os_3(CO)_{12}$ and Cab-O-Sil M5 silica (Cabot Corp., Tuscola, IL). The silica (nominal surface area 200 m^2/g) was dried at 120 °C for 24 h to remove adsorbed water. Samples containing physically adsorbed $Os_3(^{13}CO)_{12}$ were made by stirring a dichloroethane solution of $Os_3(^{13}CO)_{12}$ with silica for 2 h, followed by removal of the solvent under a stream of N_2. Thermally activated samples were prepared by refluxing $Os_3(^{13}CO)_{12}$ with silica in *n*-octane (dried over CaH_2 and distilled just prior to use) under an Ar atmosphere for 6 h, as described by Cook et al.[19] The sample was collected on a Buchner funnel, washed with methylene chloride to remove unreacted $Os_3(^{13}CO)_{12}$, and dried for 30 min by air flow. Vacuum-pyrolyzed samples were prepared from thermally activated samples by heating at 200 °C under vacuum for 4 h in a tube furnace. Our initial experiments were performed under anaerobic conditions, with samples being transferred in a N_2-filled glovebag. However, subsequent experiments indicated that identical results were obtained when samples were handled in the presence of air, indicating that such precautions were unnecessary. Infrared spectra were obtained as Nujol mulls using a Nicolet MX-S spectrophotometer.

NMR Spectroscopy. Solution ^{13}C spectra were obtained using a General Electric QE-300 NMR spectrometer. Solid-state ^{13}C NMR spectra were obtained using a home-built Fourier transform NMR spectrometer operating at 90.5 MHz.[34] Magic-angle-spinning spectra were obtained using a Doty probe (Doty Scientific, Columbia, SC). All spectra were obtained using 90° pulse excitation (typically 5–10 μs), with high-power (ca. 60 W) proton decoupling during data acquisition. To remove a broad resonance from Kel-F in the probe, background spectra obtained using empty rotors were subtracted from the spectra of the supported complexes. In some cases, spectra were also obtained using cross polarization,[35] although, as is well-known, it is difficult to obtain quantitatively reliable intensities when cross polarization is used. We estimate that the ^{13}C spin–lattice relaxation times (T_1) of the proton-containing complexes in the crystalline solid state are in the 5–30-s range, while those of the complexes that do not contain protons ($Os_3(CO)_{12}$ and $[Os(CO)_3Cl_2]_2$) are at least 1 order of magnitude longer. In contrast, the T_1's of the silica-supported complexes are relatively short. At room temperature we obtained a T_1 value of 0.77 (±0.10) s for species A (vide infra) using a saturating comb saturation-recovery method.[36] Exponential apodization (50–100 Hz) was applied to the solid-state free induction decays for sensitivity enhancement, and the digital resolution was typically 8 Hz/point. Chemical shifts are reported in ppm from tetramethylsilane with adamantane being used as an external chemical shift reference, the methine resonance being assigned a chemical shift of 29.50 ppm. The principal components of the chemical shift tensor were obtained from spinning sideband intensities by using the graphical method of Herzfeld and Berger.[37] Spectral deconvolutions were performed by using the Nicolet program NMCCAP.

Theoretical Aspects

The ^{13}C NMR spectra of solid metal carbonyls are dominated by the large chemical shift anisotropy (CSA) of the carbonyl ligand.[38] Chemical shift anisotropy refers to the orientation dependence of the chemical shift that arises when the electron distribution around the nucleus under observation has lower than tetrahedral symmetry.[39] The complete chemical shift interaction is described by a second-rank tensor δ, which is partially characterized by its three principal components, δ_{11}, δ_{22}, and δ_{33}. The average of these is the chemical shift observed in solution, termed the isotropic chemical shift (δ_i):

$$\delta_i = \tfrac{1}{3}(\delta_{11} + \delta_{22} + \delta_{33}) \quad (1)$$

In polycrystalline samples, chemical shift anisotropy gives rise to characteristic line shapes (CSA powder patterns), from which the principal components may be obtained. The width of the powder pattern is related to the chemical shift anisotropy ($\Delta\delta$), which may be defined as

$$\Delta\delta = \delta_{33} - \tfrac{1}{2}(\delta_{11} + \delta_{22}) \quad (2)$$

When the chemical shift tensor is axially symmetric, as is often the case for carbonyl ligands,[38] two of the principal components are identical, leaving only two unique components. In that case, the principal components are designated $\delta_\perp$ ($=\delta_{11} = \delta_{22}$) and $\delta_\parallel$ ($=\delta_{33}$). The deviation from axial symmetry is expressed by the asymmetry parameter (η), which may be defined as

$$\eta = \left|\frac{\delta_{22} - \delta_{11}}{\delta_{33} - \delta_i}\right| \quad (3)$$

We have used the convention that $|\delta_{33} - \delta_i| \geq |\delta_{11} - \delta_i| \geq |\delta_{22} - \delta_i|$. Chemical shift anisotropy information may be used as a tool in making peak assignments, since different functional groups have characteristic anisotropy ranges.[39] In addition, the CSA interaction provides a sensitive probe of molecular motion, since large-amplitude motions may cause partial or complete averaging.[40] The requirement for such motional averaging is that the rate of the motion be on the order of $\nu_L\Delta\delta$, where ν_L is the Larmor frequency. For typical magnetic field strengths and ^{13}C chemical shift anisotropies, this is in the 1–50-kHz range. Motions that are much faster than this are said to be in the fast limit and may produce powder line shapes with reduced anisotropies and altered asymmetry parameters.

With magic-angle spinning at a frequency much greater than $\nu_L\Delta\delta$, a single narrow resonance would be observed at the isotropic chemical shift. However, at the high magnetic field strength used in this work, this would require speeds in excess of 35 kHz, while the current limit for large samples is ca. 5 kHz. Thus, in our experiments, we are operating in the slow-spinning regime,[41] wherein the CSA powder pattern is broken up into a series of narrow spinning sidebands located at multiples of the spinning frequency on either side of a peak at the isotropic chemical shift

(30) This procedure is a modification of that reported in ref 27.
(31) Johnson, B. F. G.; Lewis, J.; Kilty, P. A. *J. Chem. Soc. A* **1968**, 2859.
(32) Calvert, R. B. Ph.D. Thesis, University of Illinois at Urbana-Champaign, 1979.
(33) Calvert, R. B.; Shapley, J. R. *J. Am. Chem. Soc.* **1977**, *99*, 5225.
(34) Walter, T. H. Ph.D. Thesis, University of Illinois at Urbana-Champaign, 1988.
(35) Pines, A.; Gibby, M. G.; Waugh, J. S. *J. Chem. Phys.* **1973**, *59*, 569.
(36) Fukushima, E.; Roeder, S. B. W. *Experimental Pulse NMR*; Addison-Wesley: Reading, MA, 1981; pp 174–176.
(37) Herzfeld, J.; Berger, A. E. *J. Chem. Phys.* **1980**, *73*, 6021.
(38) Gleeson, J. W.; Vaughan, R. W. *J. Chem. Phys.* **1983**, *78*, 5384.
(39) Veeman, W. S. *Prog. NMR Spectrosc.* **1984**, *16*, 193.
(40) Fyfe, C. A. *Solid State NMR for Chemists*; CFC Press: Guelph, Ontario, Canada, 1983; see also references cited therein.
(41) Maricq, M. M.; Waugh, J. S. *J. Chem. Phys.* **1979**, *70*, 3300.
(42) Forster, A.; Johnson, B. F. G.; Lewis, J.; Matheson, T. W.; Robinson, B. H.; Jackson, W. G. *J. Chem. Soc., Chem. Commun.* **1974**, 1042.
(43) Bryan, E. G.; Forster, A.; Johnson, B. F. G.; Lewis, J.; Matheson, T. W. *J. Chem. Soc., Dalton Trans.* **1978**, 196.
(44) Bryan, E. G.; Johnson, B. F. G.; Lewis, J. *J. Chem. Soc., Chem. Commun.* **1977**, 329.
(45) Aime, S.; Osella, D. J.; Milone, L.; Rosenberg, E. *J. Organomet. Chem.* **1981**, *213*, 207.
(46) Tachikawa, M.; Richter, S. I.; Shapley, J. R. *J. Organomet. Chem.* **1977**, *128*, C9.

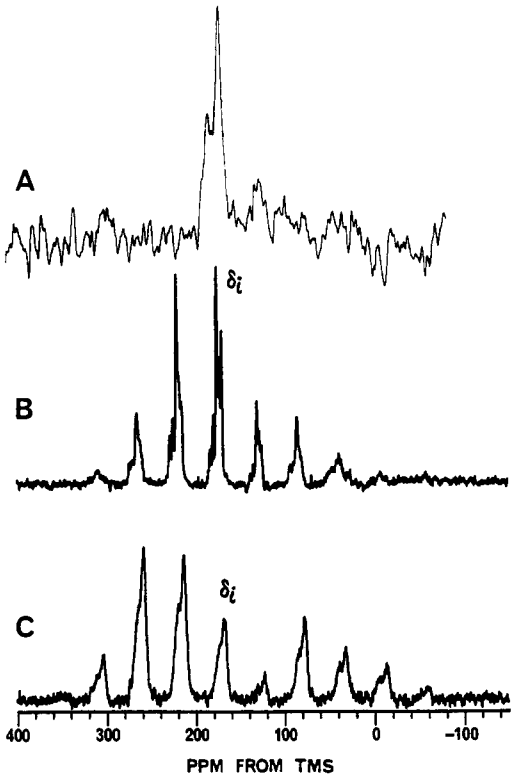

Figure 1. 90.5-MHz ^{13}C MAS NMR spectra of $Os_3(^{13}CO)_{12}/SiO_2$ samples prepared in different ways (δ_i indicates the centerband resonances): (A) impregnated sample (4.6-kHz spinning speed, 6612 acquisitions with a 5-s recycle delay); (B) sample refluxed in *n*-octane for 6 h (4.1-kHz spinning speed, 9320 acquisitions with a 2-s recycle delay); (C) sample heated at 200 °C under vacuum for 4 h (4.2-kHz spinning speed, cross-polarized using a 5-ms contact time, 16 700 acquisitions with a 2-s recycle delay).

(the so-called centerband). The centerbands are readily identified by changing the spinning speed and locating the peaks whose positions are unchanged. It has been shown[37] that the relative intensities of the spinning sidebands are related to the principal components of the chemical shift tensor, so that in the slow-spinning regime both high-resolution (δ_i) and solid-state (δ_{11}, δ_{22}, δ_{33}) information may be obtained simultaneously. We have previously demonstrated the utility of this approach for characterizing a variety of polycrystalline metal carbonyl clusters,[25] as well as a supported $Mo(CO)_5$ complex bound to alumina.[10]

Results

Typical ^{13}C MAS NMR spectra obtained for $Os_3(^{13}CO)_{12}/SiO_2$ samples prepared using different activation conditions are shown in Figure 1. For samples which have not been thermally activated (Figure 1A), we observe resonances at 183.1 and 169.9 ppm, very similar to those of $Os_3(CO)_{12}$ in solution (δ = 182.3, 170.4 ppm).[47] We thus assign these resonances to physically adsorbed $Os_3(CO)_{12}$. It appears that the axial carbonyl resonance[25] (δ_i = 183.1 ppm) is broader than the equatorial carbonyl resonance, possibly indicating a preferential interaction between the axial carbonyls and the silica surface. The absence of spinning sidebands for these resonances indicates that this species is free to undergo rapid (≫32 kHz) isotropic motion on the silica surface, completely eliminating the chemical shift anisotropy. However, these resonances are very weak in comparison to those obtained for the same sample after thermal activation, presumably because only a fraction of the $Os_3(CO)_{12}$ is present as a dispersed, physisorbed phase. The rest is believed to occur as microcrystals of $Os_3(CO)_{12}$, as previously observed by Collier et al. using electron microprobe analysis.[14] No resonances are observed from the crystalline component in the spectrum of Figure 1A because it has a spin–lattice relaxation time on the order of several hundred seconds.[25] At the relatively

(47) Aime, S.; Osella, D. *J. Chem. Soc., Chem. Commun.* **1981**, 300.

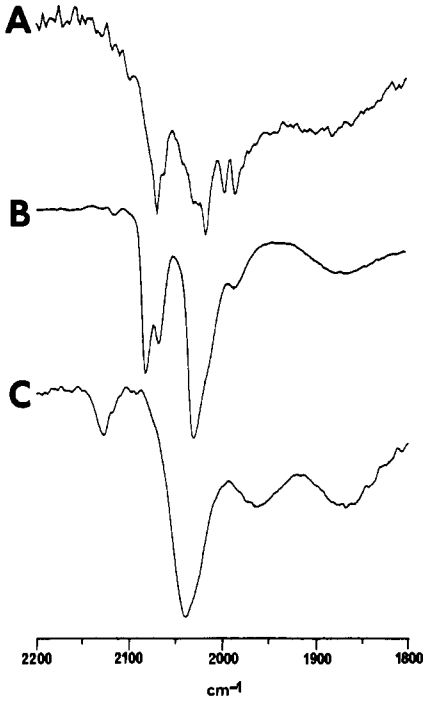

Figure 2. Infrared spectra of unenriched $Os_3(CO)_{12}/SiO_2$ samples prepared in different ways: (A) impregnated sample; (B) sample refluxed in *n*-octane for 6 h; (C) sample heated at 200 °C under vacuum for 4 h.

fast repetition rate we have used (5 s), this signal becomes saturated. With longer delay times (60 s), we have observed weak resonances attributable to crystalline $Os_3(CO)_{12}$, as evidenced by the characteristic splitting pattern and 350 ppm chemical shift anisotropy.[25] Samples prepared using unenriched $Os_3(CO)_{12}$ yield IR spectra that show the fine structure characteristic of crystalline $Os_3(CO)_{12}$, in agreement with the IR spectra reported by others (see Figure 2A).[13]

We show in Figure 1B a typical spectrum obtained for a $Os_3(^{13}CO)_{12}/SiO_2$ sample (4.0 wt % $Os_3(^{13}CO)_{12}$) that has been thermally activated by refluxing in *n*-octane (bp 125.7 °C). We also prepared samples by activation of physically adsorbed $Os_3(^{13}CO)_{12}/SiO_2$ at 150 °C under Ar, in the absence of solvent. The former method is found to give more reproducible NMR spectra and narrower resonances, possibly because the $Os_3(CO)_{12}$ concentration and temperature are more uniform throughout the sample. In both cases, however, samples prepared using unenriched $Os_3(CO)_{12}$ yield IR spectra that are similar to those reported by others (see Figure 2B).[18] The intense spinning sidebands observed in the NMR spectrum of Figure 1B indicate that the mobility of the species formed by activation at 125 °C (species A) is restricted, so that the rigid-lattice chemical shift anisotropy is partially retained. However, an analysis of the spinning-sideband intensities indicates that the anisotropies of these resonances are reduced by ca. 40% from the 370 ppm value typical of terminal carbonyl ligands in osmium clusters (vide infra). As discussed below, this partial reduction of the CSA is indicative of motional averaging.

As illustrated in Figure 3B, the centerband region of the spectrum of Figure 1B shows five distinct resonances with line widths of ca. 175 Hz (fwhh), in approximately a 1:1:4:2:2 ratio. The chemical shifts of these resonances are listed in Table I. To measure the correct relative intensities in these slow-spinning spectra, it is necessary to sum the integrals obtained for each component over all of its spinning sidebands,[25] because of significant differences in the CSA parameters of the different resonances. Since the overlap between the peaks is significant, we used spectral deconvolution to measure the relative intensities. We demonstrate in Figure 3 that the NMR spectra of thermally activated $Os_3(^{13}CO)_{12}/SiO_2$ samples prepared using a range of $Os_3(^{13}CO)_{12}$ loadings (2.5–6.0 wt %) show the same five peaks,

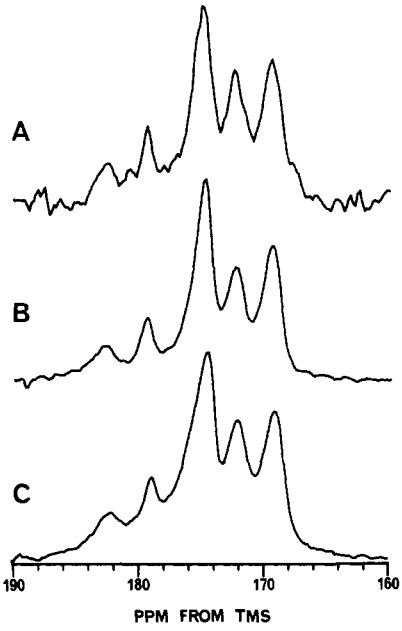

Figure 3. Expanded views of centerband resonances from 90.5-MHz ^{13}C MAS NMR spectra of $Os_3(^{13}CO)_{12}/SiO_2$ samples (refluxed in *n*-octane) with different loadings: (A) 2.5 wt % $Os_3(^{13}CO)_{12}$; (B) 4.0 wt % $Os_3(^{13}CO)_{12}$; (C) 6.0 wt % $Os_3(^{13}CO)_{12}$.

Table I. Carbon-13 Chemical Shifts of Surface and Model Species

species	δ_i,[a] ppm
$Os_3(CO)_{12}/SiO_2$ (no activation)	183.1 (1), 169.9 (1)
$Os_3(CO)_{12}/SiO_2$ (*n*-octane reflux)	182.6 (1), 179.2 (1), 174.4 (4), 172.0 (2), 169.1 (2)
$Os_3(CO)_{12}/SiO_2$ (vacuum-pyrolyzed)	167
$Os_3(CO)_{12}$[42]	182.3 (1), 170.4 (1)
$HOs_3(CO)_{10}(OCH_3)$[b]	182.3 (1), 180.8 (1), 176.8 (2), 176.3 (2), 174.0 (2), 171.7 (2)
$HOs_3(CO)_{10}(OC_6H_5)$[c]	181.6 (1), 180.4 (1), 176.1 (2), 175.5 (2), 174.5 (2), 171.6 (2)
$HOs_3(CO)_{10}(OSiEt_3)$[c]	183.3 (1), 180.5 (1), 175.9 (2), 175.2 (2), 173.0 (2), 172.1 (2)
$HOs_3(CO)_{10}(OH)$[43]	182.1 (1), 180.6 (1), 176.4 (4), 172.3 (2), 169.6 (2)
$HOs_3(CO)_{10}(O_2CH)$[b]	183.6 (1), 182.2 (1), 176.4 (2), 174.7 (2), 174.61 (2), 174.58 (2)
$HOs_3(CO)_{10}(O_2CCH_3)$[43]	186.2 (1), 184.6 (1), 178.7 (2), 177.0 (6)
$HOs_3(CO)_{10}(O_2CCF_3)$[43]	185.0 (1), 183.4 (1), 177.1 (2), 176.1 (2), 175.8 (2), 175.3 (2)
$Os_3(CO)_{10}(OCH_3)_2$[b]	181.6 (2), 181.2 (4), 178.5 (2), 170.2 (2)
$Os_3(CO)_{10}Cl_2$[44]	182.6 (2), 177.7 (4), 177.0 (2), 168.3 (2)
$H_2Os_3(CO)_{10}$[45]	182.7 (2), 181.8 (2), 176.3 (2), 175.2 (4)
$[Os(CO)_3Cl_2]_2$[c]	163.1 (1), 161.8 (2)

[a] Typical chemical shift uncertainties are ±0.1 ppm for solutions and ±0.5 ppm for solids. Numbers in parentheses are relative intensities. [b] In CD_2Cl_2. [c] in $CDCl_3$.

with similar intensity ratios. The 2.5 wt % loading is in the range typically used in previous IR and EXAFS studies: 1–2 wt % osmium,[8,14] corresponding to 1.6–3.2% $Os_3(CO)_{12}$ by weight. Our sample loadings and IR results are thus in quite good accord with those reported by others, and our NMR results do not change within the stated range of loadings.

We show in Figure 1C a typical spectrum observed for an *n*-octane-refluxed sample (4.0 wt % $Os_3(^{13}CO)_{12}$) that has been subsequently heated at 200 °C under vacuum for 4 h. As shown in Figure 2C, samples prepared in this manner from unenriched $Os_3(CO)_{12}$ yield IR spectra that are similar to those reported by others.[19] Analysis of the spinning-sideband intensities in the spectrum of Figure 1C indicates that, unlike species A, the species giving rise to these resonances (species B) is not undergoing rapid (≫32 kHz) large-amplitude motion. The centerband region from this spectrum shows a single broad (ca. 500 Hz, fwhh) resonance at 167 ppm, with an additional weak shoulder centered at 175 ppm.

Table II. Principal Components, Anisotropies, and Asymmetry Parameters of the Carbon-13 Chemical Shift Tensors for Surface and Model Species

species	δ_i, ppm	δ_{11},[a] ppm	δ_{22},[a] ppm	δ_{33},[a] ppm	$\Delta\delta$,[b] ppm	η
$Os_3(CO)_{12}/SiO_2$	183	305	208	35	−222	0.66
(*n*-octane reflux), 25 °C	179	290	204	44	−203	0.64
	174	284	205	34	−211	0.56
	172	262	206	49	−185	0.44
	169	264	180	64	−158	0.80
$Os_3(CO)_{12}/SiO_2$	175	300	283	−57	−349	0.07
(*n*-octane reflux), −105 °C						
$Os_3(CO)_{12}/SiO_2$	167	303	259	−61	−342	0.19
(vacuum-pyrolyzed)						
$Os_3(CO)_{12}$	185	312	303	−60	−367	0.04
	171	289	289	−64	−353	0.00
$HOs_3(CO)_{10}(OSiEt_3)$	183	302	302	−56	−358	0.00
	176	300	291	−62	−357	0.04
$HOs_3(CO)_{10}(OCH_3)$	186	312	312	−66	−378	0.00
	175	303	303	−81	−384	0.00
$HOs_3(CO)_{10}(OC_6H_5)$	177	305	287	−61	−357	0.08
$Os_3(CO)_{10}(OCH_3)_2$	181	310	310	−76	−386	0.00
	171	294	298	−74	−386	0.00
$H_2Os_3(CO)_{10}$	185	314	314	−72	−386	0.00
	178	305	305	−77	−382	0.00
$[Os(CO)_3Cl_2]_2$	166	304	260	−66	−348	0.19

[a] Estimated uncertainty ±10 ppm. [b] Estimated uncertainty ±20 ppm.

As mentioned above, analysis of the spinning-sideband intensities in the spectrum of Figure 1B indicates that the chemical shift anisotropies of these resonances are smaller than the ca. 370 ppm value characteristic of terminal carbonyls bound to osmium.[25,38] We summarize in Table II the CSA parameters we have measured for a variety of polycrystalline osmium carbonyl clusters. As described previously,[25] we generally use the intensities integrated over all overlapping resonances to obtain these values, except in cases where peaks are baseline-resolved. With the exception of $[Os(CO)_3Cl_2]_2$, all the compounds examined were found to have axially symmetric shielding tensors, within the experimental uncertainty (i.e. $\eta < 0.1$). The anisotropy parameters, $\Delta\delta$, fall between 348 and 386 ppm, with a mean of 370 ppm. The anisotropies observed for the carbonyl resonances of species A (see Table II) are clearly outside this range, and the shielding tensors are significantly asymmetric. However, as shown in Figure 4, when the temperature is lowered, the spinning-sideband intensities change, becoming more intense relative to the centerband. Analysis of the sideband intensities for the spectrum obtained at −105 °C (Figure 4C) indicates that the anisotropy at this temperature is 349 ppm, consistent with a rigid terminal carbonyl ligand. These results confirm that the partial reduction of the CSA observed for species A at 20 °C is due to motional averaging.

Discussion

Assignment of Species A. The reproducibility of the NMR spectra of thermally activated (refluxed in *n*-octane) $Os_3(^{13}CO)_{12}/SiO_2$ samples over a range of $Os_3(CO)_{12}$ loadings suggests that the five peaks arise from a single surface species. We have obtained the ^{13}C NMR spectra of a number of $Os_3(CO)_{12}$ derivatives that are models for the three types of structures (**1–3**) previously proposed for the chemisorbed cluster. The ^{13}C chemical shifts observed in solution are listed in Table I, and the spectra of three representative clusters are compared in Figure 5 with the spectrum of species A. In all cases, the solution spectra are consistent with the known structures of these compounds, although only partial peak assignments can be made.

Considering first the clusters of the form $HOs_3(CO)_{10}(OR)$ (**4**), six resonances are generally observed in a 1:1:2:2:2:2 ratio, consistent with their C_s symmetry. In some cases, however, fewer resonances are observed due to accidental degeneracy. For example, $HOs_3(CO)_{10}(OH)$ yields only five resonances in a 1:1:4:2:2

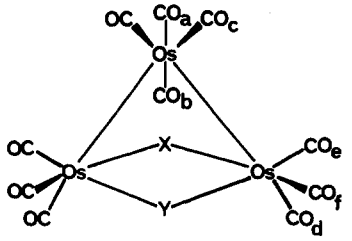

(4) X = H, Y = OR

(5) X = H, Y = O_2CR

(6) X = Y = OR

ratio.[43] The two most deshielded resonances may be assigned to sites a and b on the basis of their relative intensities. As shown in Figure 5B, for highly ^{13}C-enriched compounds these resonances appear as triplets, arising from the overlap of a singlet and a doublet. The doublet, with a splitting of 33 Hz, arises from ^{13}C–^{13}C J coupling between these two carbonyl sites, which are trans across the unique osmium atom. As previously observed,[46] $^2J_{CC}$(trans) couplings are typically much larger than $^2J_{CC}$(cis) couplings, which are only 1–5 Hz.[47] The only other resonance that can be assigned is that due to site d, which, being trans to the hydride ligand, shows a large (ca. 14 Hz) $^2J_{CH}$ coupling in the absence of proton decoupling (not shown in Figure 7).[45]

Clusters of the form $HOs_3(CO)_{10}(O_2CR)$ (**5**) have structures closely related to those of the $HOs_3(CO)_{10}(OR)$ derivatives. However, in contrast to the μ_2-OR bridging ligand, the μ_2-O_2CR bridge is almost perpendicular to the Os_3 plane, with the bridging hydride lying nearly in that plane.[29] As evident in Figure 5C, although $HOs_3(CO)_{10}(O_2CH)$ and related derivatives have C_s symmetry and thus yield six resonances in a 1:1:2:2:2:2 ratio, three of the resonances of intensity 2 have very similar chemical shifts and are thus difficult to resolve. As for the $HOs_3(CO)_{10}(OR)$ derivatives, the two most deshielded resonances can be assigned to the axial carbonyls on the unique osmium atom and again show the 33-Hz $^2J_{CC}$ splitting characteristic of carbonyls that are trans across an osmium center. In the spectrum of $HOs_3(CO)_{10}(O_2CH)$, one of the resonances at 174.6 ppm shows a 13.8-Hz $^2J_{CH}$ coupling and can thus be assigned to the carbonyls located trans to the bridging hydride (site d). The resonance at 174.7 ppm exhibits a smaller (3.9 Hz) J_{CH} coupling and is tentatively assigned to site f, which is in an equatorial position cis to the bridging hydride.

In contrast to the $HOs_3(CO)_{10}X$ structures, the dibridged derivatives, $Os_3(CO)_{10}(OR)_2$ (**6**), have C_{2v} symmetry. Consistent with this symmetry, four resonances are observed for $Os_3(CO)_{10}(OCH_3)_2$, in a 1:2:1:1 ratio, as shown in Figure 5D. Similar spectra have been observed for $Os_3(CO)_{10}Cl_2$[44] and $H_2Os_3(CO)_{10}$,[45] although for the latter derivative a 1:1:1:2 pattern is observed. In each case, the resonance of intensity 2 may be assigned to the equivalent sites d and e, and the most deshielded resonance most likely arises from the axial carbonyls on the unique osmium (equivalent sites a and b), which generally yield the most deshielded resonances. No $^2J_{CC}$(trans) coupling can occur for the latter resonances in the $Os_3(CO)_{10}X_2$ derivatives because of their equivalence. The absence of J couplings makes further assignment impossible.

It is clear that the spectrum of species A most closely resembles that of the $HOs_3(CO)_{10}(OR)$ structures and is distinctly different from the spectra of the other derivatives. Although the chemical shifts of species A differ by an average of 1.4 ppm from those of $HOs_3(CO)_{10}(OSiEt_3)$, which might be thought to be the best model, this is well within the normal range of variation observed for $HOs_3(CO)_{10}(OR)$ derivatives (see Table I). The best match for the spectrum of species A is actually the hydroxy hydride $HOs_3(CO)_{10}(OH)$, which yields chemical shifts that differ by an average of only 0.9 ppm from those of the supported cluster. It has previously been reported that the IR spectrum of $HOs_3(CO)_{10}(OH)$ is a close match to that of species A.[13] Note that our results indicate that the supported triosmium cluster possesses C_s symmetry. This is unexpected, because the silica surface should lower the symmetry, making all ten carbonyls inequivalent. This discrepancy may be resolved, however, if the supported cluster

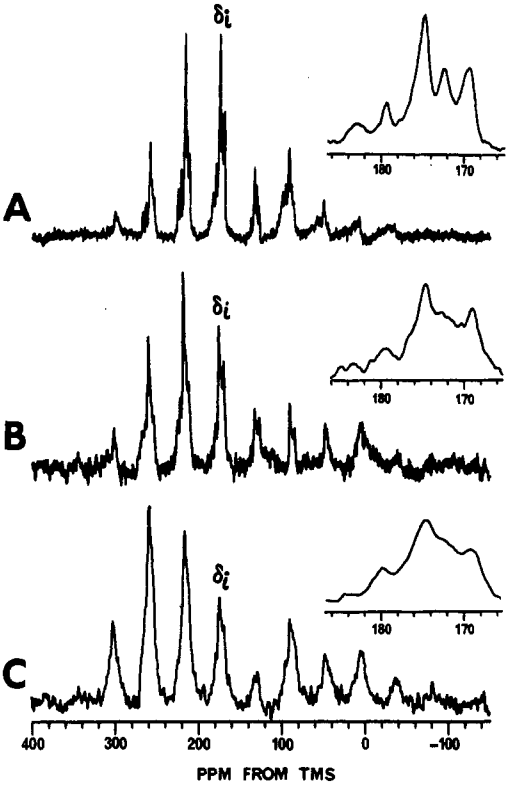

Figure 4. Variable-temperature 90.5-MHz ^{13}C MAS NMR spectra of $Os_3(^{13}CO)_{12}/SiO_2$ (refluxed in *n*-octane), with inset spectra showing expanded views of the centerband resonances: (A) 25 °C (3.8-kHz spinning speed, 3220 acquisitions with a 2-s recycle delay); (B) −63 °C (3.8-kHz spinning speed, 3140 acquisitions with a 5-s recycle delay); (C) −105 °C (3.8-kHz spinning speed, 1400 acquisitions with a 15-s recycle delay).

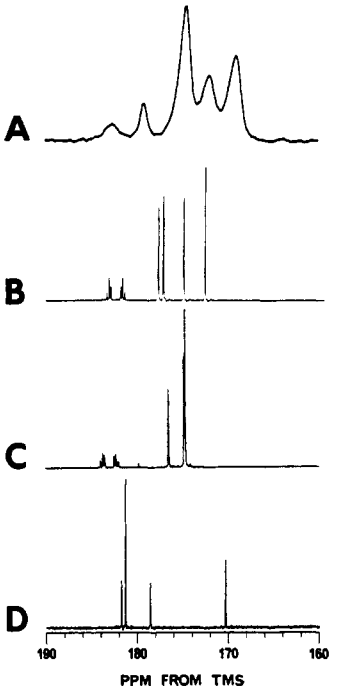

Figure 5. Comparison of the ^{13}C MAS NMR spectrum of $Os_3(^{13}CO)_{12}/SiO_2$ (refluxed in *n*-octane) and solution ^{13}C NMR spectra of model compounds: (A) MAS spectrum of $Os_3(^{13}CO)_{12}/SiO_2$ (refluxed in *n*-octane); (B) solution spectrum of $HOs_3(^{13}CO)_{10}(OCH_3)$ in CD_2Cl_2; (C) solution spectrum of $HOs_3(^{13}CO)_{10}(O_2CH)$ in CD_2Cl_2; (D) solution spectrum of $Os_3(^{13}CO)_{10}(OCH_3)_2$ in CD_2Cl_2.

has sufficient mobility to average out any surface asymmetry. Further evidence for such mobility is discussed below. In summary, our results with a large number of model compounds (Table I) strongly support structure **1** as the structure of species A.

Assignment of Species B. Vacuum pyrolysis of samples containing species A yields materials whose spectra consist of one main component, having an isotropic chemical shift of 167 ppm. We assign this peak to a second surface species, species B. However, we also observe a weaker, broad peak centered at 175 ppm. This feature is believed to be due to a small amount of residual species A that has not completely decomposed. After further vacuum pyrolysis, the intensity of this peak decreases relative to that of the 167 ppm resonance, although it is not completely eliminated even after 24 h at 200 °C. Vacuum pyrolysis of samples containing the supported triosmium cluster is believed to produce Os(II) carbonyl species with stoichiometries of $Os(CO)_2$ and $Os(CO)_3$.[13] Evidence from transmission electron microscopy[23] and IR studies of ^{13}CO-enriched samples[18] indicates that these species are most likely trimeric, although EXAFS studies show no evidence for Os–Os bonds. The osmium atoms are thus presumably linked by oxy or siloxy bridges. Recent EXAFS results on alumina-supported $Os_3(CO)_{12}$ show that each osmium has three oxygen nearest neighbors.[8] As a model for a $[Os(CO)_3(OSi{\equiv})_3]_n$ species, we have examined the dimeric carbonyl chloride $[Os(CO)_3Cl_2]_2$, which has the structure

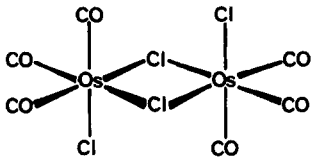

This compound is known to exist in two isomeric forms,[48] with the isomer indicated crystallizing from chloroform solution. We observe two resonances in a 1:2 ratio from $[Os(CO)_3Cl_2]_2$, consistent with C_{2h} symmetry. The resonances are shifted upfield by ca. 10 ppm from those of the triosmium clusters, due to the higher osmium oxidation state. The chemical shifts (see Table I) are in reasonable agreement with those of species B, consistent with the assignment of this species to Os(II) carbonyls. Unfortunately, since we observe only a single broad resonance for these surface species, it is impossible to draw any further conclusions. The breadth of the 167 ppm resonance (500 Hz fwhh) is nearly 3 times that of the resonances of species A, possibly because of the greater heterogeneity of these sites.

Solid-State vs Solution NMR Spectra. To assign the spectra of species A and species B, we compared the *solid-state* spectra of these supported species with *solution* spectra of model compounds. We find that the solid-state spectra of the model compounds are not as useful for purposes of comparison because lattice packing effects cause considerable peak splitting and chemical shift changes.[25,49] Since the symmetry lowering observed in the solid-state spectra is a result of the ordered crystal lattice, it should not be important for highly dispersed species attached to amorphous supports. Thus, in all cases, our assignments are based on solution ^{13}C NMR spectra, where specific intermolecular effects are absent.

Motional Averaging of Species A. The reduced anisotropies and increased asymmetry parameters of the ^{13}C chemical shift tensors of the carbonyls in species A indicate that this species is undergoing large-amplitude motions with a frequency much greater than 32 kHz. The variable-temperature results of Figure 4 show that the full rigid-lattice anisotropy is observed at −105 °C, indicating that the frequency of this motion is much slower than 32 kHz at this temperature. To account for the partially averaged chemical shift tensors observed at room temperature, we have calculated the exchange-averaged anisotropies and asymmetry parameters expected for several different types of motion. These are only approximate calculations, however, because several assumptions were made. We have assumed that the rigid-lattice tensors are axially symmetric, with the unique principal component corresponding to the C–O bond axis and that the geometry of the surface-attached cluster is similar to that of crystalline $HOs_3(CO)_{10}(OCH_3)$. This cluster was chosen because it is a close model for which accurate atomic positions were available.[50] In this crystal structure, all ten carbonyls are inequivalent, the C_s symmetry being removed by the crystal lattice. We have averaged together the values obtained for carbonyls that would be identical under C_s symmetry to facilitate comparison with the surface-attached cluster.

Table III. Calculated Motionally Averaged Anisotropies and Asymmetry Parameters of the Carbon-13 Chemical Shift Tensor for $HOs_3(CO)_{10}(OSi{\equiv})$

motion	site	θ, deg	$\Delta\delta'$, ppm	η'
free rotation	a	107.8	125	0
	b	57.9	27	0
	c	126.0	−13	0
	d	95.2	173	0
	e	128.4	−27	0
	f	40.8	−125	0
60° rotational jump	a	56.8	−231	0.52
	b	50.1	−256	0.37
	c	47.4	−265	0.32
	d	59.7	−220	0.59
	e	46.2	−269	0.30
	f	38.2	−294	0.19
72° rotational jump	a	68.0	−186	0.89
	b	59.8	−220	0.59
	c	56.3	−233	0.50
	d	71.6	175	0.94
	e	54.8	−239	0.46
	f	45.2	−272	0.28
90° rotational jump	a	84.6	175	0.28
	b	73.6	175	0.85
	c	69.2	−181	0.93
	d	89.5	175	0.03
	e	67.3	−189	0.85
	f	55.0	−238	0.47
120° rotational jump	a	111.0	−182	0.93
	b	94.4	175	0.23
	c	88.4	175	0.08
	d	119.2	−215	0.62
	e	85.5	175	0.24
	f	68.9	−182	0.93
180° rotational jump	a	144.3	−301	0.16
	b	115.9	−202	0.73
	c	108.0	175	0.93
	d	169.6	−346	0.01
	e	103.3	175	0.69
	f	81.6	175	0.44

The first model we considered is a free rotation of the triosmium cluster about the O–Si bond. We previously found evidence for rotation about the surface bond for a $Mo(CO)_5$ species attached to γ-Al_2O_3.[10] For free rotation, the motionally averaged chemical shift tensors are axially symmetric ($\eta' = 0$) and have reduced anisotropies ($\Delta\delta'$):[35]

$$\Delta\delta' = \tfrac{1}{2}(3\cos^2\theta - 1)\Delta\delta$$

The reduction factor is governed by the angle (θ) formed by the individual C–O bonds relative to the rotation axis. The angles and corresponding motionally averaged CSA parameters calculated on the basis of this model are listed in Table III. For this calculation, we used the anisotropy of −349 ppm measured for species A at −105 °C. The calculated values are clearly not in agreement with the experimental results, indicating that the surface-attached cluster is not undergoing free rotation about the surface bond.

We also considered exchange mechanisms. There have been reports of localized carbonyl exchange processes occurring at both

(48) Bruce, M. I.; Cooke, M.; Green, M.; Westlake, D. J. *J. Chem. Soc. A* **1969**, 987.

(49) (a) Dorn, H. C.; Hanson, B. E.; Motell, E. *J. Organomet. Chem.* **1982**, *224*, 181. (b) Hasselbring, L.; Lamb, H.; Dybowski, C.; Gates, B.; Rheingold, A. *Inorg. Chim. Acta* **1987**, *127*, L49.

(50) Churchill, M. R.; Wasserman, H. J. *Inorg. Chem.* **1980**, *19*, 2391.

the unique and the nonunique osmium atoms in $Os_3(CO)_{10}XY$ clusters in solution at elevated temperatures (>70 °C).[43,44] Neither mechanism, however, would account for the observation that all of the carbonyl resonances have reduced anisotropies. In addition, the centerband expansions shown in Figure 4 indicate that the positions of the peaks are largely invariant with temperature, ruling out carbonyl exchange between inequivalent sites. All of the resonances do broaden as the temperature is lowered, and the peak at 172.0 ppm appears to split. This may be due to a reduction in the symmetry of the cluster, caused by a decrease in the rate of motion. That is, if the apparent C_s symmetry of the surface-attached cluster is due to motional averaging, slowing the motion should produce the expected C_i symmetry. The spectrum should then contain ten resonances, instead of six.

The third type of motion considered is a two-site rotational jump, involving alternation of the cluster between two orientations by rotation about the surface bond. Such hindered rotation occurs when there are local minima in the barrier for rotation. One well-known example of this type of motion is the flipping (180° rotational jump) of the phenyl rings of phenylalanine.[51] For a rotational jump, the motionally averaged chemical shift tensor is the average of the tensors for the two interconverting orientations,[52] labeled A and B:

$$\boldsymbol{\delta}' = {}^1/_2(\boldsymbol{\delta}^A + \boldsymbol{\delta}^B) = \begin{pmatrix} \delta'_{xx} & \delta'_{xy} & 0 \\ \delta'_{xy} & \delta'_{yy} & 0 \\ 0 & 0 & \delta'_{zz} \end{pmatrix}$$

where

$$\delta'_{xx} = {}^1/_2[\delta_\parallel(1 + \cos^2\theta) + \delta_\perp \sin^2\theta]$$

$$\delta'_{xy} = {}^1/_2(\cos\theta)(\sin\theta)\Delta\delta$$

$$\delta'_{yy} = {}^1/_2[\delta_\perp(1 + \cos^2\theta) + \delta_\parallel \sin^2\theta] \qquad \delta'_{zz} = \delta_\perp$$

$\delta_\perp$ and $\delta_\parallel$ are the principal components of the rigid-lattice chemical shift tensor, and θ is the angle formed by the C–O bond vectors of the two orientations of each site. The principal components of the exchange-averaged tensor are obtained by diagonalizing this matrix. From these values the motionally averaged chemical shift anisotropies and asymmetry parameters are calculated using eqs 2 and 3. Using the anisotropy of −349 ppm obtained from the −105 °C spectrum of Figure 4, the only unknowns are the angles θ for the six sites. These angles may be calculated for a rotational jump by any angle about the O–Si bond of the cluster, using $HOs_3(CO)_{10}(OCH_3)$ as a structural model. We list in Table II the angles θ and the calculated motionally averaged CSA parameters for rotational jumps of $360°/n$ (n = 2–6). These calculations show that the rotational-jump model, in general, produces highly asymmetric tensors ($\eta > 0$), in agreement with the experimental results. In addition, the range of anisotropies calculated for jump angles of 90 and 120° (175–238 ppm) are in reasonable agreement with the experimental anisotropies (158–222 ppm). It is difficult to compare the experimental and calculated values exactly, because the peak assignments are largely uncertain (vide supra). In addition, one of the peaks (δ_i = 174.4 ppm) is a composite of two overlapping resonances that likely have different CSA parameters. Thus, it is impossible to specify the jump angle with any precision. However, this is clearly the best of the models considered. That rotation about the surface bond might be restricted appears to be consistent with recent computer models for the $HOs_3(CO)_{10}(OSi{\equiv})$ cluster.[53] On the basis of the assumption that the silica surface may be modeled using low-index planes of β-cristobalite, that study showed that some of the carbonyl ligands are directed toward the surface, in close contact with neighboring silanol groups. A large-angle jump may be required to avoid strong steric repulsion as the cluster rotates about the surface bond.

Finally, we note one puzzling aspect to our results. As may be seen from Figure 4, as the temperature is lowered, the CSA of species A increases, but there is no major loss of intensity which would be expected due to solely a decrease in the rate of motion. That is, the spectrum does not appear to go through an intermediate-exchange regime. Rather, our results suggest that the jump angle decreases with decreasing temperature. Whether this is physically reasonable or not would require a more detailed understanding of the dynamic structure of species A than is currently available. Use of other motional models, such as wobbling in a cone, with a decreasing cone angle at lower temperature, while at first attractive, has the difficulty that it would yield axially symmetric chemical shift tensors at all temperatures. Thus, while we are confident about the assignment of species A to structure **1**, there remains some uncertainty as to the actual motional behavior of this species, and the problem is underdetermined.

Conclusions

The results described above demonstrate that it is possible to obtain highly resolved ^{13}C NMR spectra of surface-attached metal carbonyl clusters through the use of magic-angle spinning and high magnetic field strengths. Our results confirm that the initial chemisorption product formed by the reaction of $Os_3(CO)_{12}$ with silica is a species of the form $HOs_3(CO)_{10}(OSi{\equiv})$, in agreement with the gas evolution measurements of Psaro et al.[13] In contrast to earlier IR and EXAFS investigations, our study shows that ^{13}C NMR spectroscopy can readily distinguish between the three types of structure postulated for this surface-attached cluster. With this sensitivity to subtle differences in cluster structure, ^{13}C NMR spectroscopy should become a valuable addition to the growing number of techniques for characterizing supported metal complexes.

In addition to the information provided by isotropic chemical shifts, the chemical shift anisotropy parameters calculated from the spinning-sideband intensities have revealed new features of the mobilities of supported osmium carbonyl species. We have shown evidence for a physisorbed $Os_3(CO)_{12}$ species with solution-like mobility. In addition, our results suggest that the surface-attached cluster undergoes rapid large-angle rotational jumps about the surface bond. This rotational mobility should not be possible for $Os_3(CO)_{10}(OSi{\equiv})_2$ or $HOs_3(CO)_{10}(O_2Si{=})$ species (structures **2** and **3**) attached to the surface by two bonds. Thus our CSA data provide further evidence that the initial chemisorption product has the $HOs_3(CO)_{10}(OSi{\equiv})$ structure. In contrast to the mobility of the initial chemisorption product, the Os(II) carbonyl species formed by vacuum pyrolysis are found to be immobile on the 10^{-5}–10^{-4}-s time scale. This is consistent with models indicating that these species are bound by two or three surface oxygens.

Acknowledgment. This work was supported by National Science Foundation Grants DMR 88-14789 (E.O., Solid State Chemistry Program) and DMR 86-12860 (J.R.S., through the University of Illinois Materials Research Laboratory).

Supplementary Material Available: Simulated chemical shift anisotropy powder pattern and 90.5-MHz ^{13}C MAS NMR spectrum of $Os_3(^{13}CO)_{12}$ (2 pages). Ordering information is given on any current masthead page.

(51) (a) Frey, M. H.; DiVerdi, J. A.; Opella, S. J. *J. Am. Chem. Soc.* **1985**, *107*, 7311. (b) Kinsey, R. A.; Kintanar, A.; Oldfield, E. *J. Biol. Chem.* **1981**, *256*, 9028.

(52) Spiess, H. W. *Chem. Phys.* **1974**, *6*, 217.

(53) Hsu, L.-Y.; Shore, S. G.; D'Ornelas, L.; Choplin, A.; Basset, J.-M. *Polyhedron* **1988**, *7*, 2399.